Nonlinear Dynamics **13:** 39–57, 1997.

Phase-Space Reconstructions and Stick-Slip

B. F. FEENY
Department of Mechanical Engineering, Michigan State University, A231 Engineering Building, East Lansing, MI 48824, U.S.A.

J. W. LIANG
Department of Mechanical Engineering, MingChi Institute of Technology, Taipei, Taiwan, R.O.C.

(Received: 4 June 1996; accepted: 17 September 1996)

Abstract. Nonsmooth processes such as stick-slip may introduce problems with phase-space reconstructions. We examine chaotic single-degree-of-freedom stick-slip friction models and use the method of delays to reconstruct the phase space. We illustrate that this reconstruction process can cause pseudo trajectories to collapse in a way that is unlike, yet related to, the dimensional collapse in the original phase-space. As a result, the reconstructed attractor is not topologically similar to the real attractor. Standard dimensioning tools are applied in effort to recognize this situation. The use of additional observables is examined as a possible remedy for the problem.

Key words: Phase-space reconstructions, stick-slip, method of delays, friction oscillators, nonsmooth systems.

1. Introduction

When running experiments, it is not typically feasible to measure all of the active states in the system. To compensate for this, there are methods for estimating the system behavior in the full state space from a small number of measured observables. These methods involve phase-space reconstructions. The reconstruction of the full state space is useful in system characterization, nonlinear prediction, and in estimating bounds on the size of the system [1, 2].

The *method of delays* (described below) is the most common method for reconstructing the phase space. This method has been justified for smooth systems by Takens' embedding theorem [3], which states that, if basic hypotheses are satisfied, applying the method of delays to an observable produces a trajectory in the reconstructed or pseudo phase space which is a topological embedding of the trajectory in the real phase space. The important implication is that the limit set in the real space is mapped injectively to the reconstructed phase space.

We consider the application of this method to mechanical systems with stick-slip dynamics. A "stick" is defined as an event in which a relative velocity is zero for a finite interval of time. Stick-slip systems represent a class of mechanical systems with interesting dynamical properties [4]. These properties arise from the fact that stick-slip is associated with a nonsmooth process. Stick-slip studies are applicable to robotics, vehicular squeak and squeal, cutting processes, and earthquake prediction.

A stick-slip system does not have the smoothness required for Takens' embedding theorem, and can consequently cause the method of delays to fail. In particular, stick-slip can lead to a singularity when mapping the observed time history into a higher dimensional space [5].

Phase-space reconstructions are often performed on experimental systems for which the model is unknown. If a nonsmooth event occurs without notice, poor results may be unsuspiciously obtained.

An example of this failure can be visualized by imagining a history of sampled relative displacements x_n, which, during a stick, are momentarily constant. Suppose, for example, we were to reconstruct the phase space in three dimensions. According to the method of delays, we build vectors (x_n, x_{n+l}, x_{n+2l}), where l is a delay index. (If h is the sampling interval, then $\tau = hl$ is the delay time.) However, during a sticking interval, it is possible that the points $x_n = x_{n+l} = x_{n+2l} = x_{\text{stick}}$, and that the two points (x_n, x_{n+l}, x_{n+2l}) and $(x_{n+1}, x_{n+1+l}, x_{n+1+2l})$, for example, might both be the same point as $(x_{\text{stick}}, x_{\text{stick}}, x_{\text{stick}})$. Thus, when we plot the reconstructed vectors, many of them pile up on the identity line. (If l were large, however, x_n, x_{n+l}, and x_{n+2l} could span a time interval greater than the sticking time, and this problem is avoided. On the other hand, if l is too large, the delayed coordinate may become statistically independent of the reference coordinate. There are prescribed methods for finding good values of l in smooth systems.)

In this example, the reconstructed phase space is fundamentally different than the real phase space. The resulting map which takes the real phase-space manifold M_p into the reconstructed manifold M_r is not invertible, and thus not an embedding. The subsequent dimensionality study fails. This translates to inaccurate models and poor characterizations and predictions. For example, log-log plots of correlation integrals *versus* box size may not produce the expected straight-line characteristic [5, 6].

There are two problems to address here. First, we would like to detect when a reconstruction problem of this nature occurs in a "black-box" experiment. Next, when there is a reconstruction problem, we need to make adjustments to relieve it, so that the rest of the dimensionality study may continue.

This paper is organized as follows. In the next section, we simulate two single-degree-of-freedom models which provide a visual illustration of the problem. In Section 3, we apply three tests to the reconstructed data and look for symptoms of singularities in the reconstruction. In Section 4, we show that the addition of an observable will, in some cases, unfold the singularities. Section 5 contains some remarks, and conclusions are offered in Section 6.

2. Example Stick-Slip Oscillators

Effects similar to stick-slip can happen in many types of systems, including those with dry [7] or lubricated friction [8], plastic members [9], sliding-mode controllers [10], impacts [11, 12], and even superconductors [13]. In this paper, we focus on oscillators with dry friction. We look at two forced mass-spring systems, one with a fixed contact and one on a moving belt, the mechanics models of which are shown in Figure 1.

2.1. Model I

The first example (Model I) has been examined experimentally and analytically [5, 14, 15]. Neglecting the transverse component of the normal load, the nondimensional equation of motion is of the form

$$\ddot{x} + 2\zeta\dot{x} + x + n(x)f(\dot{x}) = a\cos\Omega t, \tag{1}$$

where x is the displacement, ζ is the damping ratio, and $a\cos\Omega t$ represents a harmonic excitation. $f(\dot{x})$ represents the coefficient of friction, and, using the Coulomb model, is given by

$$f(\dot{x}) = \mu\,\text{sign}(\dot{x}), \quad \dot{x} \neq 0, \qquad -1 \leq f(\dot{x}) \leq 1, \quad \dot{x} = 0. \tag{2}$$

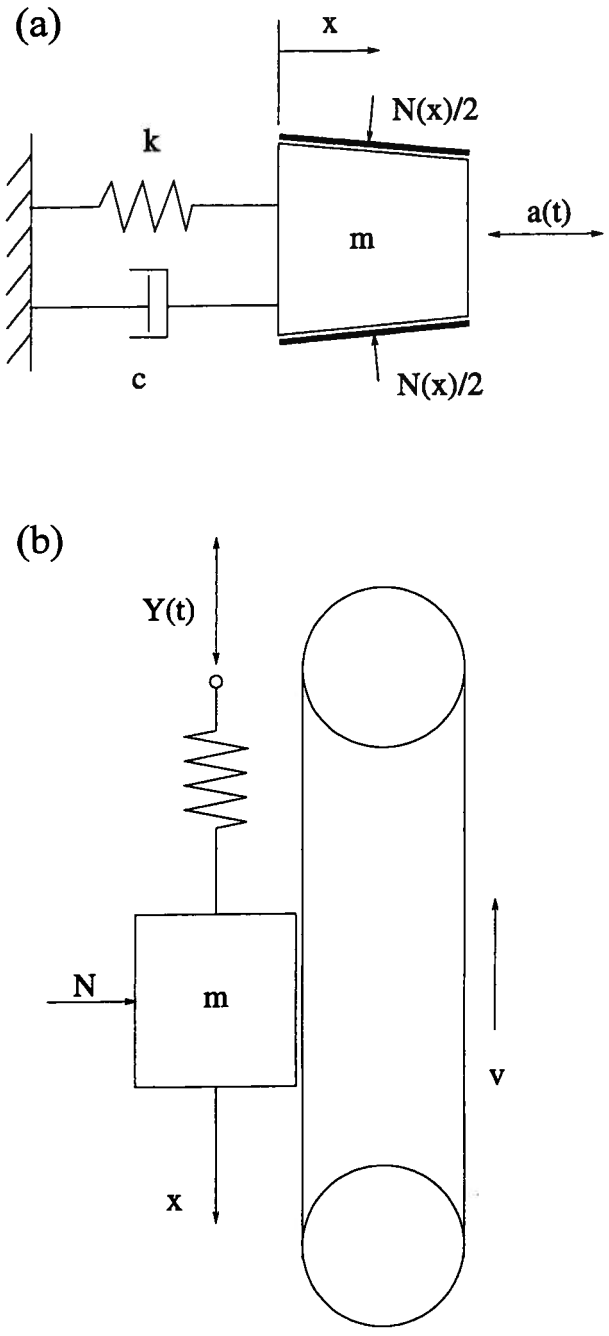

Figure 1. Mechanics models for two stick-slip oscillators. (a) Model I, (b) Model II.

The wedge shape gives rise to a spring-loaded normal load given by $n(x) = 1 + k_n x$ for $x > -1/k_n$, and $n(x) = 0$ for $x < -1/k_n$ when the contact is lost. If the model had a bilateral contact, there would always be a nonnegative normal load, and the friction model would be such as in the oscillator studied by Anderson and Ferri [16].

This paper focuses on the case in which the static and kinetic friction coefficients are the same ($\mu = 1$). This simplification is not always unreasonable, and the instabilities associated with $\mu < 1$ are not necessary in generating chaos. The structure of the state space for this oscillator is $R^2 \times S^1$. The circle S^1 represents the periodicity in the explicit time variable.

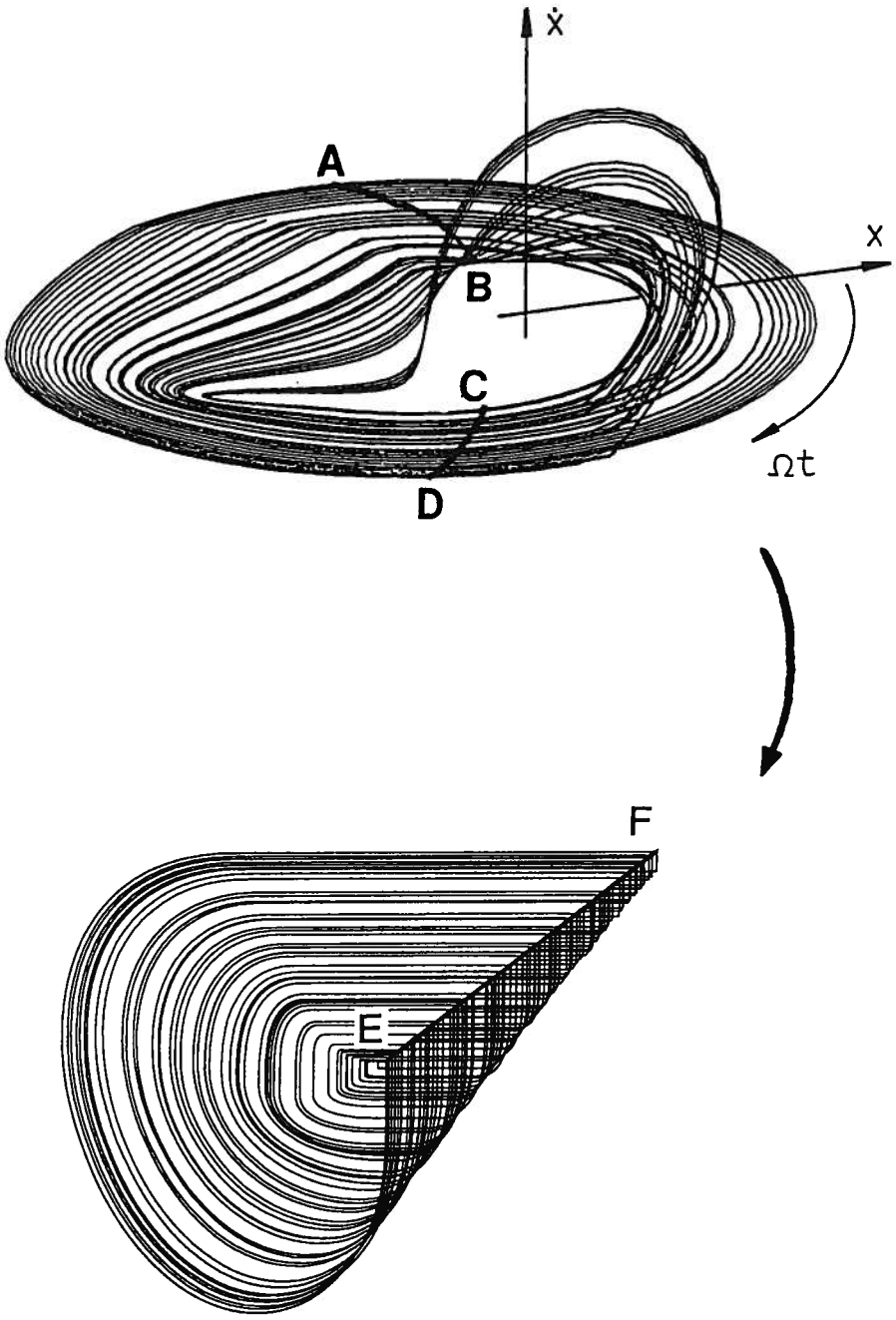

Figure 2. Above is a numerical solution of Model I with $\Omega = 1.25$, $a = 1.9$, and $k_n = 1.5$. Below is the reconstruction, illustrating the collapse which takes place.

There is a surface of discontinuity on the plane defined by $\dot{x} = 0$. The displacement axis is parallel to this surface, and the velocity axis is normal to it.

The numerical integration must account for the discontinuity. Our integration scheme closely follows that of Shaw [17] and Feeny and Moon [15]. This results in data with a nonuniform sampling rate, which was then interpolated into data with a constant sampling rate for the analyses.

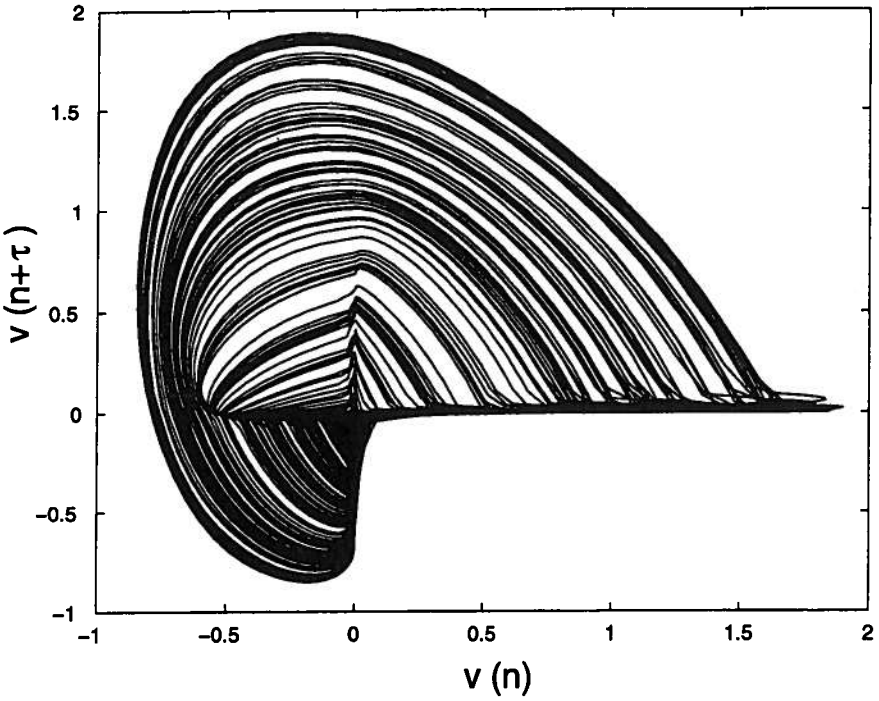

Figure 3. A phase-space reconstruction based on the observed velocity in Model I leads to a collapse of trajectories onto a point at the origin. The time delay, chosen for illustration, is $\tau = 1.15$ in nondimensional time units, almost a quarter period.

For a range of values of a and Ω, the oscillator is chaotic. An example of a chaotic solution to Equation (1) is shown in Figure 2 for the parameter values $k_n = 1.5$, $a = 1.9$, and $\Omega = 1.25$. The figure represents a projection of a three-dimensional phase portrait in cylindrical coordinates. The radial coordinate is the displacement, the circumferential coordinate is $\phi = t(\mathrm{mod}\, 2\pi/\Omega)$, and the longitudinal coordinate is $\dot{x}$. Trajectories travel clockwise in the figure. The numerical simulation fits well with experimental observations in a mass-beam system with friction applied in the same way [15].

The geometry of this flow has been examined in detail [5]. For the parameter values given in Figure 2, sticking can occur anywhere in a finite subinterval of ϕ. For the given parameter values, trajectories undergo some stick during every cycle of excitation. Sticking is associated with a complete contraction, or collapse, in the state space. This dimensional collapse leads to a flow on a 2-D branched manifold, and to one-dimensional Poincaré-map dynamics.

The pseudo phase space was reconstructed from the displacement history using the method of delays. The delay time was $\tau = 1.15$, chosen to illustrate the collapsing effect rather than by a rigorous method based on mutual information [18] or autocorrelation [19]. The action of this reconstruction is depicted in Figure 2. A region of sticking trajectories between AB and CD has effectively been collapsed onto the identity line EF in the pseudo phase space.

When the observable is chosen to be the velocity rather than the displacement, the collapsing in the reconstructed attractor is more severe, since all of the sticking samples have the value of zero. Such a phase-space reconstruction, with $\tau = 1.15$, is displayed in Figure 3.

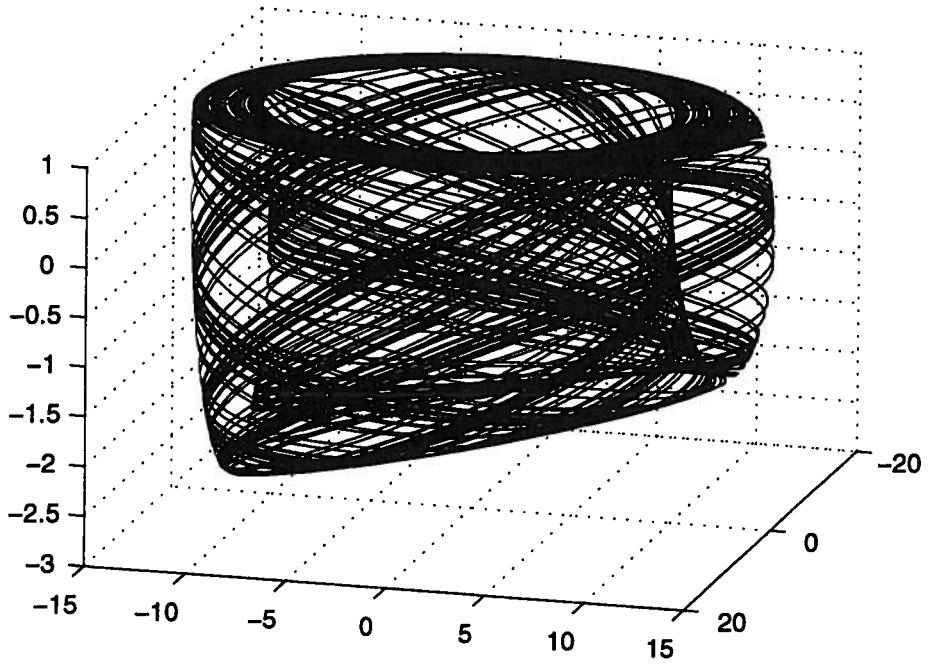

Figure 4. A numerical solution of Model II. The radial coordinate is the displacement, the circumferential coordinate is $\phi = t(\mathrm{mod}\, 2\pi/\Omega)$, and the longitudinal coordinate is $\dot{x}$. Trajectories travel clockwise.

2.2. MODEL II

Somewhat similar features arise in the forced, belt-driven oscillator (Model II) studied by Popp and Stelter [6] and Popp et al. [20]. The equation of motion is

$$\ddot{x} + x + x_s + f_r(v_r) = Y\cos(\Omega t). \tag{3}$$

Here, v represents the belt velocity, $v_r = \dot{x} - v$ is the relative velocity between the mass and the belt, and Y and Ω are the amplitude and frequency of base motion. The friction model used was of the form $f_r = N\mu(v_r)\,\mathrm{sign}(v_r)$, where N is the ratio between the normal load and spring stiffness, and $\mu(v_r) = (\mu_0 - \mu_1)/(1 + \lambda|v_r|) + \mu_1 + \alpha v_r^2$. Finally, $x_s = \mu(v)N$ is the static equilibrium position. The parameters used in this study are $\mu_0 = 0.4$, $\mu_1 = 0.1$, $\lambda = 1.42$ s/m, $\alpha = 0.7$ s^2/m^2, $N = 1.0$ m, $v = 1.0$ m/s, $Y = 0.5$ m, and $\Omega = 2.1625$ rad/s. The friction coefficient $\mu(v_r)$ has a negative slope for a range of values of v_r up to about 2 m/s. This oscillator has underlying one-dimensional map dynamics, with intermittency and period doubling as a routes to chaos [20]. The flow is on a 2-D manifold.

A projection of the three-dimensional phase portrait is shown in Figure 4. Using the method of delays, the two-dimensional projections of the reconstructions are exhibited based on the observed displacement history and the observed velocity (Figure 5). Here, the time delay is based on the first zero crossing of the autocorrelation function.

The singularity in the reconstruction occurs in a slightly different way as in the first example. Again, pseudo trajectories collapse onto a line during some phases of the flow. But here the iterates enter the line at one end, march along the line, and exit at the other end.

To explain this, we consider a three-dimensional pseudo phase space, and plot displacement points (x_n, x_{n+l}, x_{n+2l}). If all three points are involved in the same sticking event, they can be rewritten as $(x_n, x_n + hlv, x_n + 2hlv)$, where h is the sampling interval. The ith iterate of

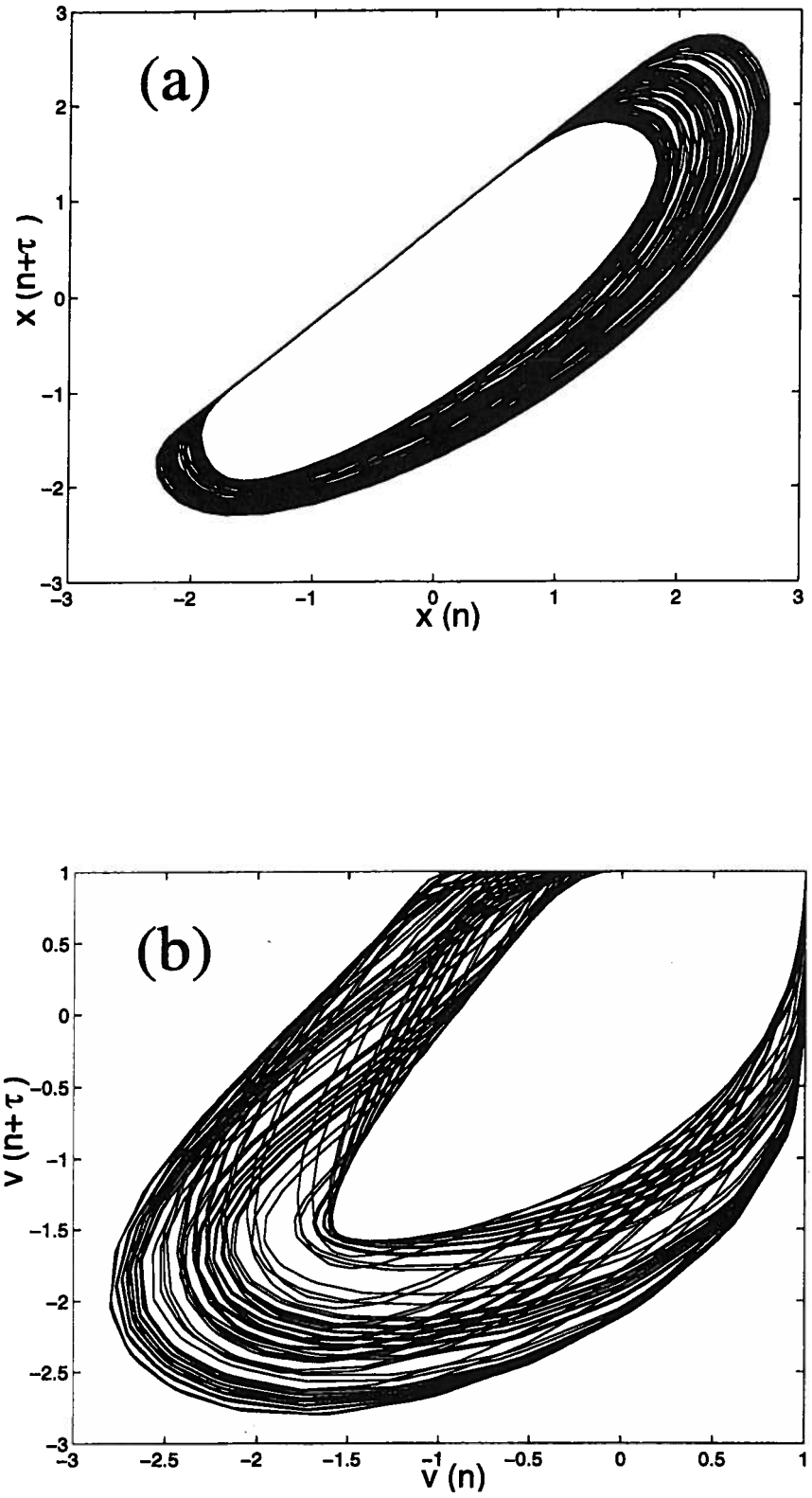

Figure 5. (a) A phase-space reconstruction based on the observed displacement in Model II leads to a collapse of trajectories onto a line parallel to the identity. (b) A phase-space reconstruction based on the observed velocity in Model II leads to a collapse of trajectories onto a point off of the origin.

this pseudo phase point is $(x_n + hvi, x_n + lhv + hvi, x_n + 2lhv + hvi)$, provided that the sticking event lasts through this iterate. The ith iterate defines a line parallel to the identity line, parameterized by i with a rate of hv. Later, another sticking event may occur for the trio $(x_m, x_m + hlv, x_m + 2hlv)$ and its jth iterate $(x_m + hvj, x_m + lhv + hvj, x_m + 2lhv + hvj)$, which defines a line parallel to the identity, parameterized by j at a rate of hv. At $j = (x_n - x_m)/hv$, the latter line has the value of the initial point of the former line. Thus these parallel lines coincide, and all sticking trios are collapsing on the same line.

3. Diagnosis of Reconstruction Singularities

We would like to be able to identify a singularity in the mapping from the observable history to the pseudo phase space, should one occur. Properties of Models I and II are that, in the reconstruction, trajectories experience a collapse from a two-dimensional manifold to a one-dimensional manifold, and then spread out again into the two-dimensional manifold. In the continuous-time sense, this is a singularity. In the discretized sense, Model I results in singularities, in that reconstructed points pile up, while Model II results in an artificially created increase in density of points in a lower-dimensional manifold.

We can apply standard analysis tools which examine the nearness of pseudo phase points, and seek special features which might point to evidence of singularities. To this end, we analyze the data for false nearest neighbors [1] (FNN), recurrent trajectories [21–23], and we also test for the dependence of number of "ε nearest neighbors" on the delay time.

The designed application of the FNN test is in the determination of the correct embedding dimension. The idea is that if the embedding dimension is too small, portions of the strange limit set will cross over itself. As the dimension of the reconstruction is increased, these false crossings unfold. Thus, if the nearest neighbor of a pseudo phase point reconstructed in dimension d_E suddenly becomes far away when the reconstruction dimension is increased, then it will have been considered a false nearest neighbor. In this work, a nearest neighbor is labeled "false" if $R_{d_E+1}/R_{d_E} > 15$, where R_{d_E} is the distance between the points in the d_E-dimensional reconstruction space. When a dimension is reached in which there are essentially no false nearest neighbors, then the appropriate embedding dimension is found. A healthy system usually has some robustness in the determination of the embedding dimension d_E under variations in other parameters, such as the delay time.

Recurrences in the trajectory are typically identified when trying to extract unstable periodic orbits.

Examples of these tests on the Duffing oscillator are given previously [24] as an example of a smooth system.

Most of our analyses have been done on 8000–10000 data points sampled from phase trajectories which are confined to a 2-D manifold. Larger data sets would produce more precise results, but the illustrated features should be well represented.

3.1. Symptoms in Model I

First we consider the effect of increasing the dimension of the reconstruction from d_E to $d_E + 1$, while holding the time delay fixed. The two pseudo vectors are

$$\mathbf{y}_{d_E} = (x_n, x_{n+l}, \ldots, x_{n+l(d_E-1)}) \quad \text{and} \quad \mathbf{y}_{d_E+1} = (x_n, x_{n+l}, \ldots, x_{n+l(d_E-1)}, x_{n+ld_E}).$$

For some values of l and d_E, there will be sticking points for which both $\mathbf{y}_{d_E}$ and $\mathbf{y}_{d_E+1}$ contain elements which all stick. However, there will be some sticking points for which the

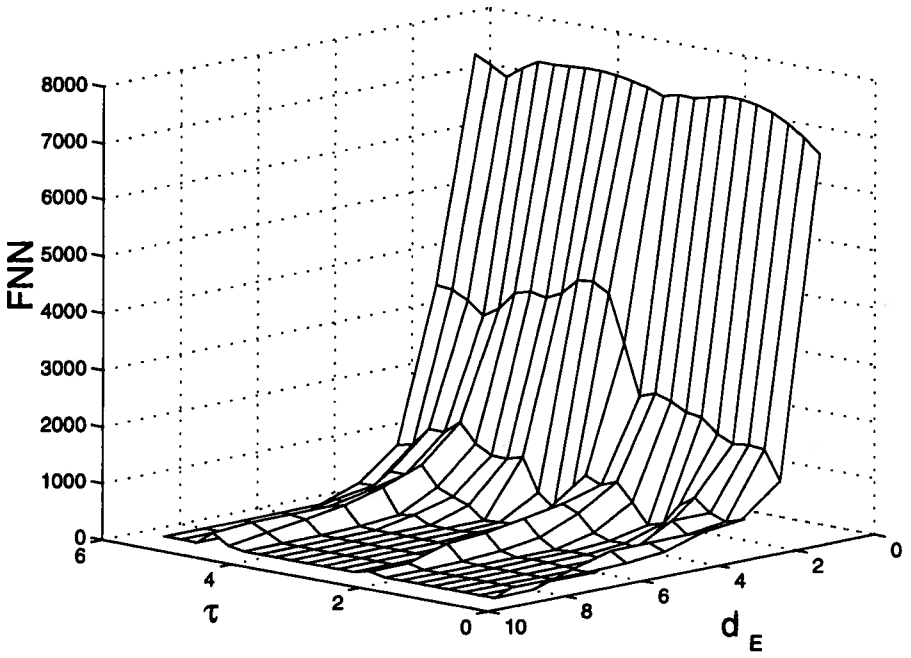

Figure 6. The number of false nearest neighbors *versus* the delay index and the dimension of the pseudo phase space for reconstructions of Model I.

added delay element (the x_{n+ld_E} term) is no longer sticking, bringing the pseudo phase point off of the identity line of collapse. The FNN test might identify such events as an unfoldment. When a dimension d_E is reached such that x_n and $x_{n+(d_E-1)l}$ are spaced apart in time to an extent at which both points cannot be sticking, then all pseudo phase points will be off of the identity, and no unfoldments will occur in this sense. However, if the delay index l is commensurate with the sticking phase, all dimensions d_E will lead to pseudo phase points with all sticking elements (although, in this case, the collapse line is no longer the identity line).

An example of the FNN test on 8000 displacement samples from Model I in Figure 6 has features which correspond to the discussion above. For different values of delay time, the FNN test reveals a different reconstruction dimension for which unfoldments cease. There is also a ridge of persisting false nearest neighbors for delay times which are nearly commensurate with the driving period.

Noting that the value of the delay influences the number of collapsing pseudo phase points, we tested the number $N(\varepsilon)$ of "ε nearest neighbors" *versus* the delay time, while holding d_E fixed. The number of ε nearest neighbors was defined by the number of points $\mathbf{y}$ in the reconstructed attractor whose nearest neighbors fall within a ball of size ε centered at $\mathbf{y}$. In other words, we find the nearest neighbor for each point $\mathbf{y}$ in the reconstructed attractor, and check whether it lies within an $\dot{\varepsilon}$-ball centered at $\mathbf{y}$. If so, the total is incremented. The total number $N(\varepsilon)$ is plotted *versus* the delay time. Figure 7, based on 9099 displacement samples, shows that for values of delay time which are commensurate with the driving period, there are large numbers of ε nearest neighbors. These are due to collapsing points which are not just near, but in fact lie on top of each other. Although not shown, $N(\varepsilon)$ decreases as the ball size decreases.

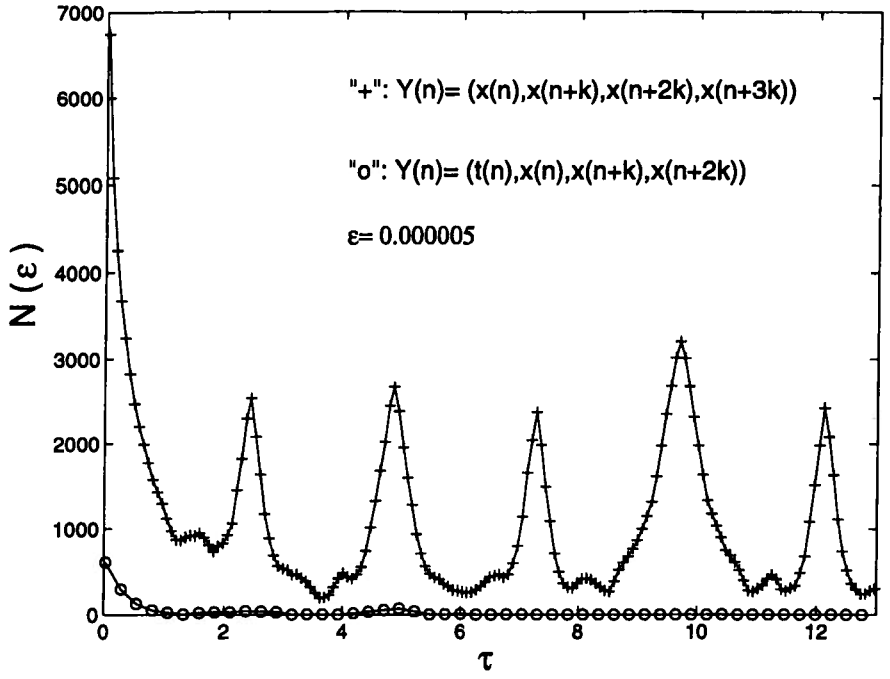

Figure 7. The number $N(\varepsilon)$ of ε nearest neighbors *versus* delay time τ for a four-dimensional reconstruction of Model I (+ symbols). The 'o' symbols refer to a reconstruction based on three delays in the displacement in addition to the phase angle ϕ.

Finally, we employ a recurrence test for extracting the unstable periodic orbits from the chaotic attractor. The idea is, given a reconstruction, we look for near periodicities by examining the distance between a point $\mathbf{x}_n$ and its iterates $\mathbf{x}_{n+r}$. If $\|\mathbf{x}_n - \mathbf{x}_{n+r}\| < \varepsilon$, where ε is some prescribed small value, then the points are considered to be part of a nearly periodic trajectory of period rh. Typically ε is taken as 0.005 times the span of the attractor [22, 23]. We then plot the number of recurrences *versus* r. In a smooth system, the recurrence plot shows spikes at values of r corresponding to the periods of unstable periodic orbits.

If the nearly periodic orbit passes through the collapsing identity line, we would expect the recurrence test to detect the points which pile up there. Hence, we would expect a range of recurrences centered at true periodicities, which in this case are multiples of the excitation period. This feature is drawn out in Figure 8, which is based on 25000 displacement samples. The recurrences near period zero also occur from pile-ups. The range of recurrences tends to narrow as the reconstruction dimension increases and the number of collapsed points decreases.

We would typically require the appropriate embedding dimension prior to applying the recurrence test. However, results of the FNN test suggest that it may be difficult to determine the embedding dimension in the face of reconstruction singularities; in fact, the appropriate embedding dimension may not make sense if the embedding cannot take place. If a reconstruction dimension is chosen so that it is slightly low, false recurrences take place where trajectories cross, showing up on the recurrence plot as a low-level, noisy set of spikes for all r. As long as the reconstruction dimension is not exceedingly small, these events are few in number compared to the true recurrences [24].

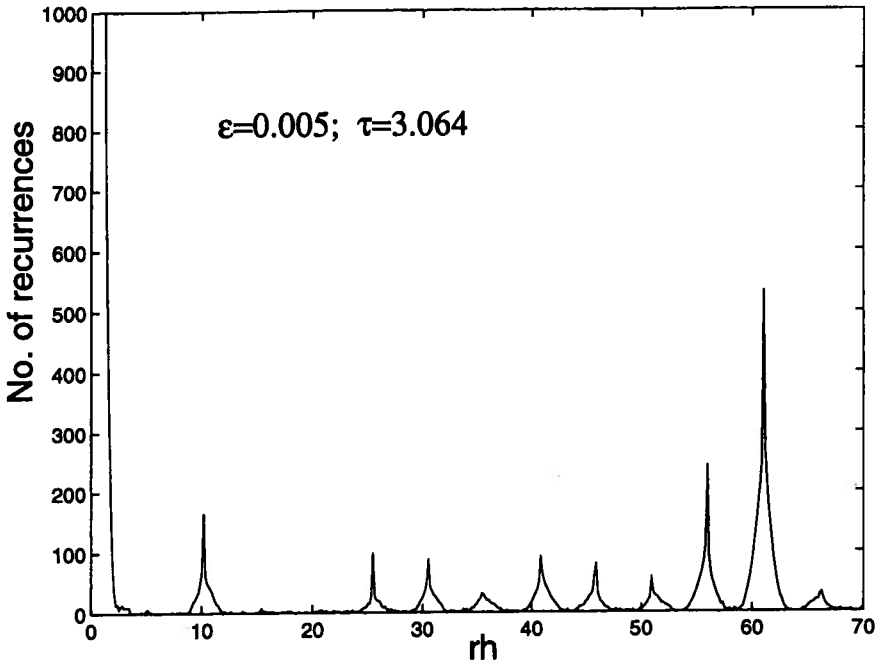

Figure 8. The number of recurrences *versus* the delay time rh for a 2-D reconstruction of Model I.

3.2. Symptoms in Model II

Features of this model which distinguish it from the above model are that the sticking interval can be centered at any phase angle of excitation, and that the singularities in the reconstruction make it so trajectories march along the line, and do not pile up on stationary points.

We apply these three tests to Model II when reconstructed from the displacement history. The FNN test applied to 10000 displacement samples (Figure 9) shows that the unfolding of false nearest neighbors is quite dependent on the delay time. (In smooth systems, there may be a subtle dependence as such.) The patterned ridges do not occur since sticking can occur at any phase interval, and thus there is no pattern of commensurability with the excitation period.

The near neighbors test reveals no striking features in this plot, probably because there are no pure pile-ups of points in the reconstruction space.

The recurrence test (Figure 10), applied to 18000 displacement samples, exposes bands of periodicities, rather than in pure multiples of the driving period. In this case, a single periodic orbit with sticking will consist of a portion in which points are marching on the collapse line. This single, isolated periodic orbit would itself indicate the correct periodicity. However, nonperiodic segments of a long sampled trajectory also interact with the collapse line, and hence interfere with time-delayed segments of itself. This artificial recurrence is caused by the reconstruction collapse. It gives birth to false periodic orbits (periodic in the reconstruction space based on recurrences on the collapse line, but not periodic in the real phase space) with periods slightly incommensurate with the driving period. The recurrence test detects these false periodicities.

When we reconstruct the phase space from the velocity signal, the reconstruction singularities are more severe, and lead to collapse points. Figure 11 shows an FNN test based on 10000 velocity samples, revealing an erratic structure with some dependence of the suggested

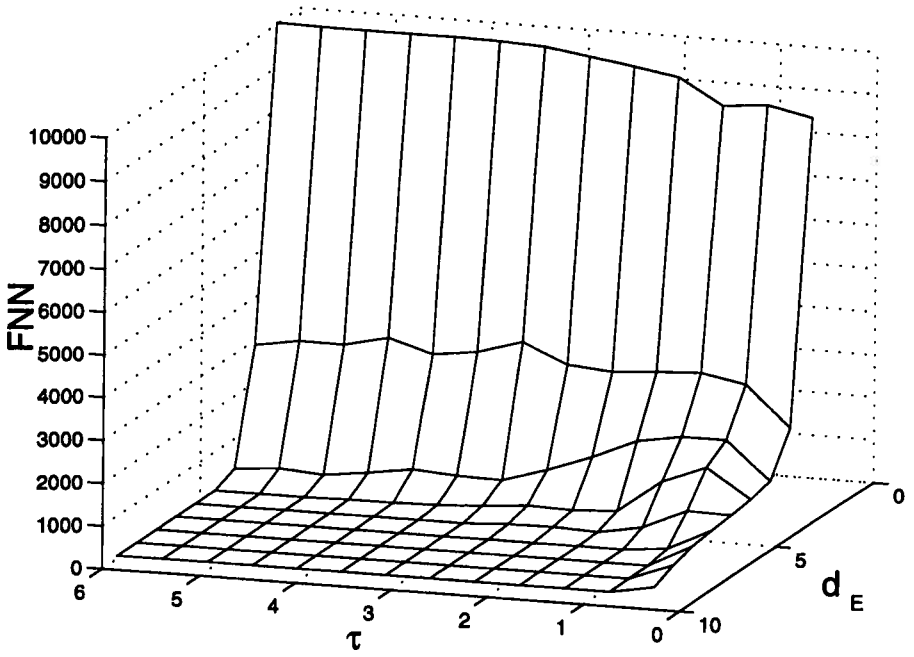

Figure 9. The number of false nearest neighbors *versus* the delay index and the dimension of the pseudo phase space for reconstructions of Model II.

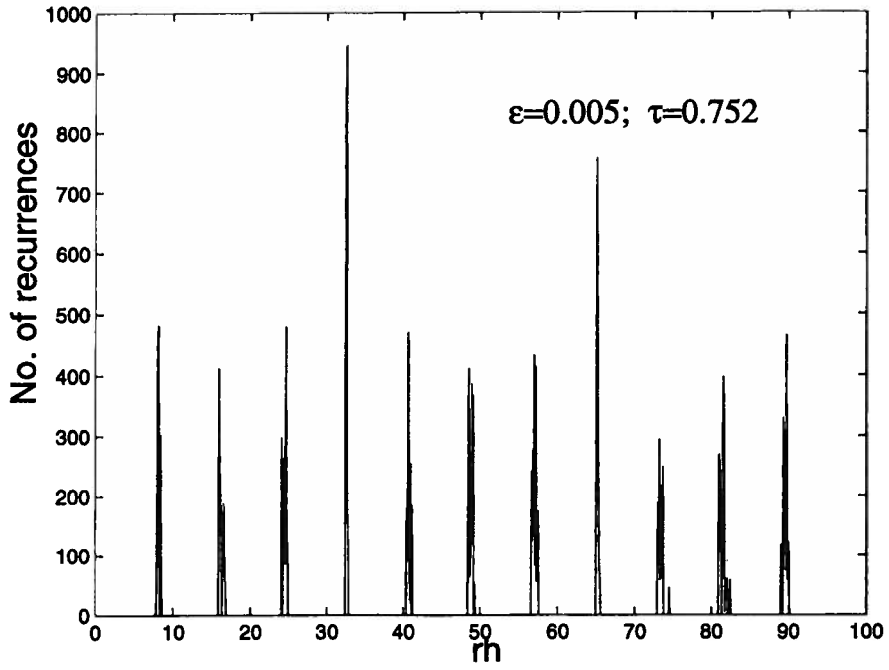

Figure 10. The recurrence plot in a 2-D reconstruction shows bands of periodicities centered at multiples of the driving period. These off-period recurrences indicate the presence of false periodic orbits. The quantity rh is the delay time of the recurrence search.

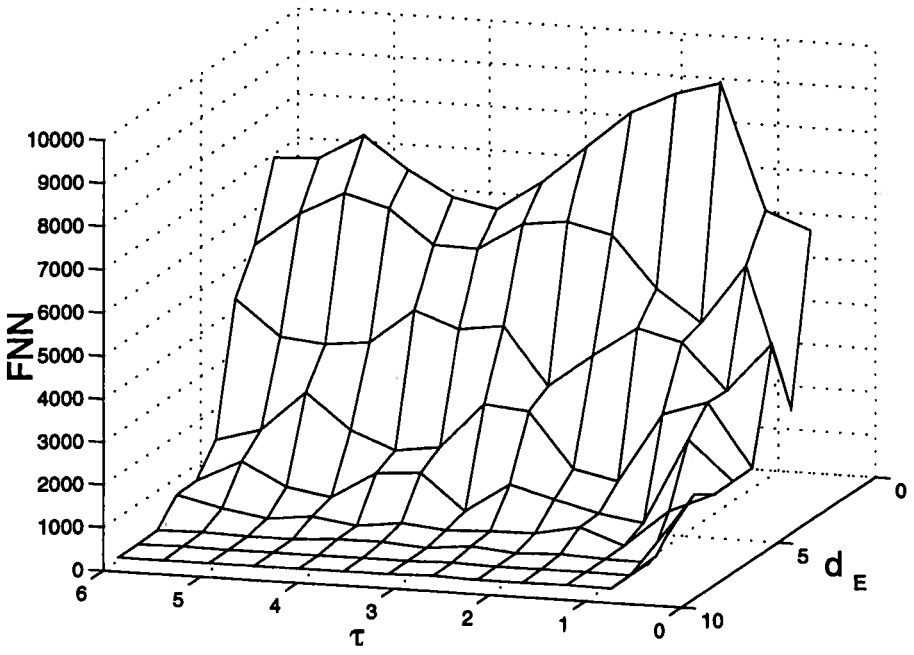

Figure 11. The FNN test for a reconstruction of Model II.

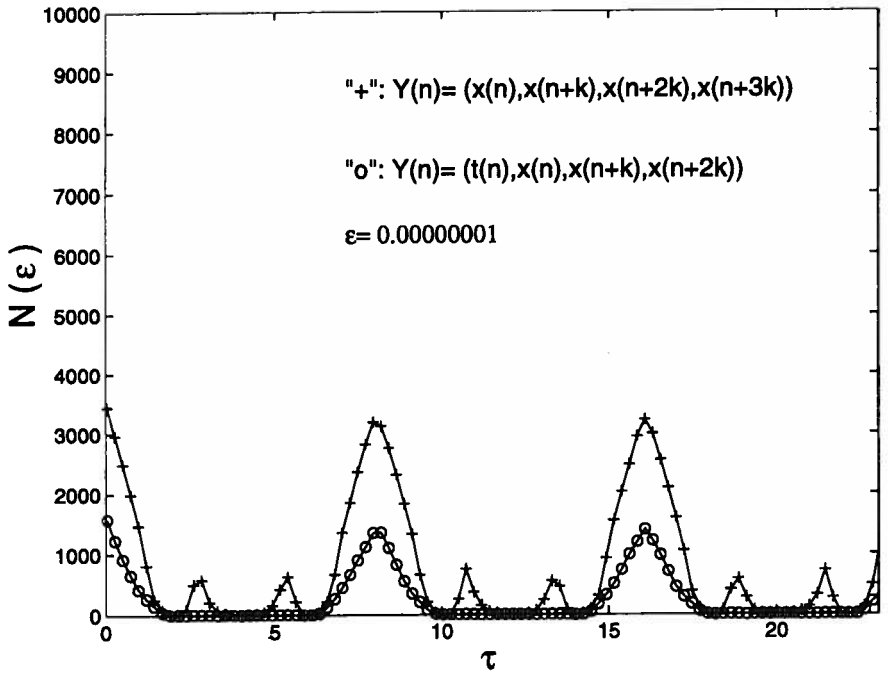

Figure 12. The ε-nearest-neighbors test for a reconstruction of Model II. The + signs indicate the result from a reconstruction with only this observable. The 'o' signs indicate the result from a reconstruction with ϕ and delays of the velocity history.

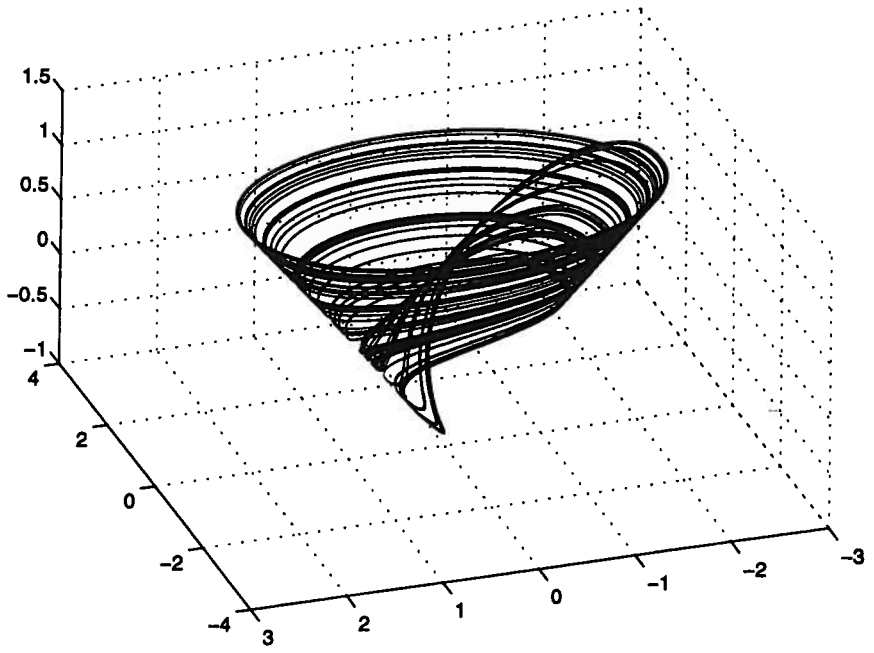

Figure 13. A projection of the three-dimensional reconstruction for Model I based on the observed displacement and ϕ. The radial and longitudinal coordinates are x_n and x_{n+l}, while the circumferential coordinate is ϕ_n.

embedding dimension on the delay index. Figure 12 indicates large numbers of ε nearest neighbors for delay indices which are not commensurate with the driving period. The severity of the collapse of the reconstruction trajectories to a single point gives rise again to large numbers of reconstruction points which are not only near, but lie on top of each other. The plot was generated from 10000 velocity samples.

4. Reconstruction with an Additional Observer

Once we have a reconstruction problem, we would like be able to make some modifications so that the reconstruction is an embedding. This might involve choosing a delay time such that the reconstructions work, if possible. The choice of τ, however, may turn out to be nonoptimal in terms of other aspects of the dynamics. We might try to implement changes in the reconstruction method. In this work, we use an additional observer by incorporating the phase of the driver, ϕ, into the reconstruction to unfold the singularities. (Increasing the number of observables has been shown to improve phase-space reconstructions in a convection problem [25].)

For the collapsing pseudo phase points of Model I, keeping track of the time index of each point provides a way to distinguish the points. The reconstructed points can be plotted with the phase angle, as visualized in the three-dimensional reconstruction depicted in Figure 13. The figure is plotted in cylindrical coordinates such that x_n is the radial coordinate, x_{n+l} is the longitudinal coordinate, and $t(\mathrm{mod}\, 2\pi/\Omega)$ is the radial coordinate.

Similarly, in Model II, adding the phase angle to the reconstruction coordinates unfolds two points on the collapse line. Since two reconstructed trajectories in the collapse line will have entered the line at different initially sticking points, they will be associated with different

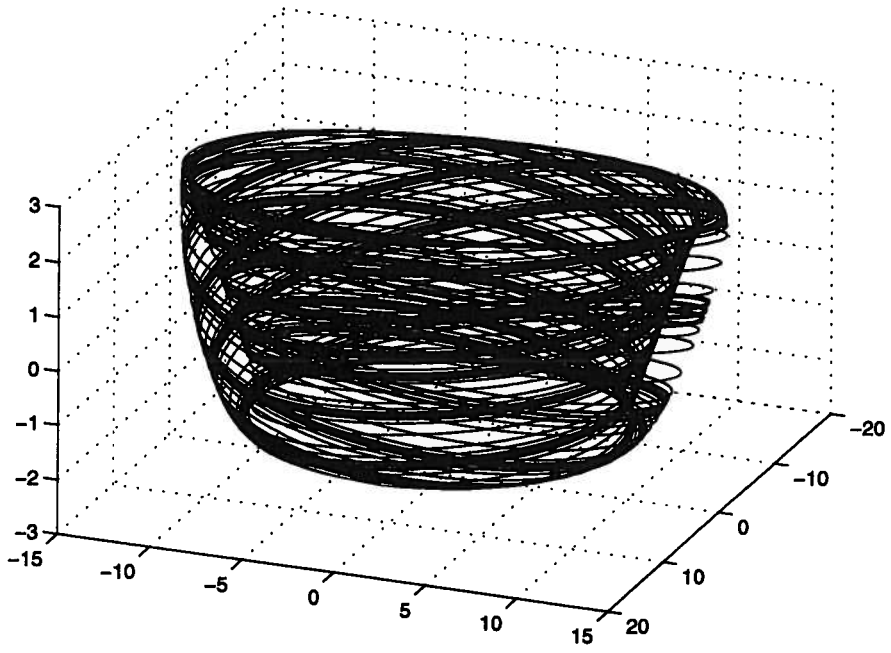

Figure 14. A projection of the three-dimensional reconstruction for Model II based on the observed displacement and ϕ. The radial and longitudinal coordinates are x_n and x_{n+l}, while the circumferential coordinate is ϕ_n.

time indices (the i and j indices discussed in Section 2) and will thus be unfolded. This is visualized in Figure 14, which is plotted in cylindrical coordinates.

Knowing that the reconstructions with the displacement and time variables are good, the analysis tests employed in the previous section are now applied to these new phase space reconstructions. Since these tests employ balls, we normalized the time axis to be of the same span as the displacement axes. The FNN test shows a "healthy" characteristic in each oscillator, indicating that, depending on τ, a reconstruction dimension of three or four, including two or three delayed displacement coordinates, is sufficient for an embedding (Figure 15). Figures 15a and b are based on 8000 and 10000 displacement samples.

Referring back to Figure 7, the plot with the 'o' symbols indicates that the large numbers of ε nearest neighbors at values of delay indices commensurate with the driving period is greatly reduced by adding the time variable ϕ to the reconstruction. The total dimension of this reconstruction is four, including three delays of the displacement history.

We have not performed a recurrence test here, since the $\phi = t(\mathrm{mod}\, 2\pi/\Omega)$ variable will automatically separate the nonharmonics of the driving period.

However, when using the velocity as an observable, the addition of the time variable serves to unfold the collapse points into collapse lines of the "marching" type. It is insufficient to produce an embedding. A symptom of this would appear as an erratic characteristic in the FNN test on Model II with delays on the velocity in conjunction with ϕ. Also, there are values of τ which lead to large $N(\varepsilon)$, as shown in Figure 12 by the 'o' symbols.

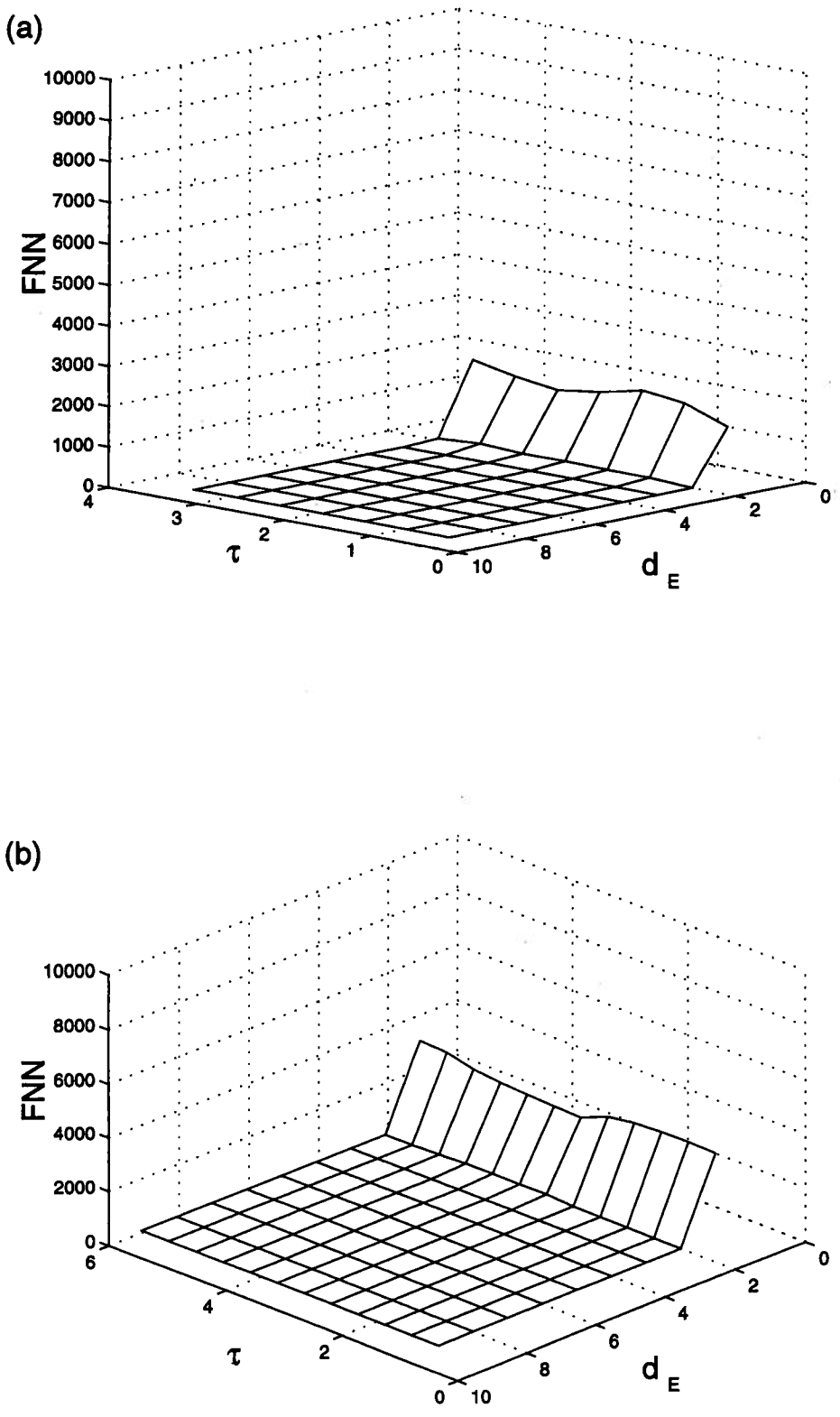

Figure 15. FNN tests on a trajectory reconstructed from delays on sampled displacements along with ϕ reveal healthy characteristics in (a) Model I and (b) Model II. Here, d_E is the number of delay coordinates, so that the dimension of the reconstructed phase space, including the phase coordinate, is $d_E + 1$.

5. Remarks

Models I and II were used to motivate a discussion on how phase-space reconstructions can fail in these kinds of nonsmooth systems, how the failure can be diagnosed using nonlinear signal processing tools, and how the addition of an observer might be one way to fix the problem. Are these ideas going to extend to more complicated systems? If so, for what types of problems will they be useful? A package of techniques applicable to a wide range of systems, ranging from autonomous to nonautonomous, low dimensional to high dimensional, and point contact to distributed contact, would be desirable.

In expanding the applicability of these ideas, it may be necessary to apply other analysis tools, or to develop new techniques. The analysis tools used here were based on metric ideas, i.e. distances within balls. The purpose was to use these metric quantities to indicate the occurrence of crossing or collapsing trajectories. Other analysis tools might be applicable. For example, redundancy analysis [18] deals with the "sharpness of conditional probability distributions." Collapsing orbits should have some effect on the probability distributions of a partitioned phase space. Topological considerations such as knots [26] and relative rotation rates [23, 27], when confronted with distinct periodic cycles collapsing together in a reconstruction, may lead to another diagnostic tool for 3-D reconstructions. Also, the correlation integral has led to unusual features in the presence of stick-slip [5, 6]. We have not looked into whether the features of the correlation integral make some sense in terms of the known dynamical structures of the simple oscillators of this study.

The choice of the appropriate delay time has been a serious issue addressed by many researchers. In this paper, we have used delay times which have been chosen to illustrate the failures of the reconstruction. The reconstructions for Model II have been done with time delays at or near the first zero crossing of the autocorrelation function. There might be interesting relationships between the usage of accepted tools and the degree of reconstruction failure.

Finally, we have chosen our observers based on loose discussions. For experiments in which a nonsmoothness is suspected a priori, it would be helpful to have a theoretical foundation relating the orientation, dimension, and number of discontinuities to the choices of observers and additional observers. In Models I and II, an observed velocity leads to problems which are more severe than with an observed displacement. The velocity-based reconstruction would need two additional observables to remedy the singularity problem. In these cases, the displacement axis is parallel to the plane of discontinuity, while the velocity axis is normal to it.

Effects in multi-degree-of-freedom systems were hinted at in a previous paper [24]. Observing the displacements of the masses which stick can lead to problems, while observing the displacement of another mass might be acceptable. Complications may increase by increasing the number of contacts, such as in a model of an earthquake fault [28]. Multiple contacts imply multiple planes of discontinuity in the phase space.

Would a discontinuity in the displacement field cause any phase-space reconstruction problems? An impact oscillator can undergo a dwell, which is essentially a stick, which would lead to problems similar to those discussed here. An impact model consists of a differential equation for some parts of the flow, and a difference equation for the impact law; additional kinds of reconstruction problems cannot be ruled out.

In our examples, we added the excitation phase angle to the displacement observer. Had we added velocity, we would not have unfolded the attractor since the velocity had the same value

associated with each sticking point. A general rule which assists us in choosing additional observers would be beneficial.

6. Conclusion

We have examined the phase-space reconstructions of two examples of forced oscillators with chaotic stick-slip motion. Using the method of delays, there is a potential for the reconstructions to have singularities, and thus fail to produce sets in pseudo phase space that are embeddings of their counterparts in the real phase space. The FNN test, a recurrence test, and a near-neighbors test together flagged defects in the reconstruction. Other tools might lead to further diagnostic tests.

A remedy for the problem was to add the excitation phase angle to the reconstruction. For the case of an observed displacement, this resulted in visually acceptable portraits, and analytical tests with healthy characteristics.

The next step would include applying these ideas to more complicated models, and also developing a theory which assists us in choosing observables. It would also be worthwhile to examine experimental systems and systems with noise.

Diagnosing reconstruction failures may be of importance since, in an experimental system without a model, nonsmooth behavior may not be suspected. It would be beneficial to detect blemishes in a phase-space reconstruction, and furthermore, to cure them if possible so that further analyses can take place. This would aid us in modeling nonsmooth processes, which might include cutting processes, vehicular squeak, robot joints, and earthquake dynamics.

References

1. Kennel, M., Brown, R., and Abarbanel, H. D. I., 'Determining embedding dimension for phase-space reconstruction using a geometrical construction', *Physical Review A* **45**, 1992, 3403–3411.
2. Abarbanel, H. D. I., Brown, R., Sidorowich, J., and Tsimring, L., 'The analysis of observed chaotic data in physical systems', *Reviews of Modern Physics* **65**, 1993, 1331-1392.
3. Takens, F., 'Detecting strange attractors in turbulence', in *Dynamical Systems and Turbulence*, D. A. Rand and L. S. Young (eds.), Lecture Notes in Math., Vol. 898, Springer, 1981, pp. 366–381.
4. Feeny, B., 'The nonlinear dynamics of oscillators with stick-slip friction', in *Dynamics with Friction*, A. Guran, F. Pfeiffer, and K. Popp (eds.), World Scientific, 1996, pp. 36–92.
5. Feeny, B., 'A nonsmooth Coulomb friction oscillator', *Physica D* **59**, 1992, 25–38.
6. Popp, K. and Stelter, P., 'Stick-slip vibrations and chaos', *Philosophical Transactions of the Royal Society of London A* **332**, 1990, 89–105.
7. Marui, E. and Kato, S., 'Forced vibration of a base-excited single-degree-of-freedom system with Coulomb friction', *Journal of Dynamic Systems, Measurement, and Control* **106**, 1984, 280–285.
8. Polycarpou, A., and Soom, A., 'Transitions between sticking and slipping at lubricated line contacts', in *Friction-Induced Vibration, Chatter, Squeal, and Chaos*, ASME Winter Annual Meeting, DE-Vol. 49, 1992, pp. 139–148.
9. Pratap, R., Mukherjee, S., and Moon, F. C., 'Dynamic behavior of a bilinear hysteretic elasto-plastic oscillator, parts I and II', *Journal of Sound and Vibration* **172**, 1994, 321–358.
10. Utkin, V. I., 'Variable-structure systems with sliding mode control', *IEEE Transactions on Automatic Control* **22**, 1973, 212–222.
11. Kowalik, Z. J., Franaszek, M., and Pierański, P., 'Self-reanimating chaos in the bouncing-ball system', *Physical Review A* **37**, 1988, 4016–4022.
12. Cusumano, J. P. and Bai, B.-Y., 'Period-infinity periodic motions, chaos, and spatial coherence in a 10 degree-of-freedom impact oscillator', *Chaos, Solitons and Fractals* **3**(5), 1993, 515–535.
13. Moon, F. C., 'Chaotic vibrations of a magnet near a superconductor', *Physics Letters A* **132**(5), 1988, 249–252.
14. Feeny, B. and Moon, F. C., 'Autocorrelation on symbol dynamics for a chaotic dry-friction oscillator', *Physics Letters A* **141**(8–9), 1989, 397–400.
15. Feeny, B. and Moon, F. C., 'Chaos in a dry-friction oscillator: experiment and numerical modeling', *Journal of Sound and Vibration* **170**, 1994, 303–323.

16. Anderson, J. R. and Ferri, A. A., 'Behavior of a single-degree-of-freedom system with a generalized friction law', *Journal of Sound and Vibration* **140**(2), 1990, 287–304.
17. Shaw, S. W., 'On the dynamic response of a system with dry friction', *Journal of Sound and Vibration* **108**, 1986, 305–325.
18. Fraser, A. M. , 'Reconstructing attractors from scalar time series: A comparison of singular system analysis and redundancy criteria', *Physica D* **34**, 1989, 391–404.
19. Broomhead, D. S. and King, G. P., 'Extracting qualitative dynamics from experimental data', *Physica D* **20**, 1986, 217–236.
20. Popp, K., Hinrichs, N., and Oestreich, M., 'Analysis of a self-excited friction oscillator with external excitation', in *Dynamics with Friction*, A. Guran, F. Pfeiffer, and K. Popp (eds.), World Scientific, 1995, pp. 1–35.
21. Auerbach, D., Cvitanovic, P., Eckmann, J.-P., Gunaratne, G., and Procaccia, I., 'Exploring chaotic notion through periodic orbits', *Physical Review Letters* **58**, 1987, 2387–2389.
22. Lathrop, D. P. and Kostelich, E. J., 'Characterization of an experimental strange attractor by periodic orbits', *Physical Review A* **40**, 1987, 4028–4031.
23. Tufillaro, N. B., Abbott, T., and Reilly, J., *An Experimental Approach to Nonlinear Dynamics and Chaos*, Addison-Wesley, New York, 1992.
24. Feeny, B. F. and Liang, J. W., 'Phase-space reconstructions of stick-slip systems', in *Proceedings of the ASME 1995 Design Engineering Technical Conferences, 3A*, ASME DE-Vol. 84-1, 1995, 1061–1070.
25. Read, P. L., 'Phase portrait reconstruction using multivariate singular systems analysis', *Physica D* **69**, 1993, 353–365.
26. Holmes, P. and Ghrist, R., 'Knotting within the gluing bifurcation', in *Nonlinearity and Chaos in Engineering Dynamics*, J. M. T. Thompson and S. R. Bishop (eds.), Wiley, Chichester, 1994, pp. 299–315.
27. Tufillaro, N. B., Solari, H. G., and Gilmore, R., 'Relative rotation rates – fingerprints for strange attractors', *Physical Review A* **41**, 1990, 5717–5720.
28. Carlson, J. M. and Langer, J. S., 'Mechanical model of an earthquake fault', *Physical Review A* **40**(11), 1989, 6470–6484.